IEEE Access
Multidisciplinary ⋮ Rapid Review ⋮ Open Access Journal

Received 7 June 2023, accepted 19 June 2023, date of publication 3 July 2023, date of current version 13 July 2023.

Digital Object Identifier 10.1109/ACCESS.2023.3291411

RESEARCH ARTICLE

A New Approach Based on Balancing Composite Motion Optimization and Deep Neural Networks for Spatial Prediction of Landslides at Tropical Cyclone Areas

TRAN ANH TUAN[1,2], PHAN DONG PHA[1,2], TRAN THI TAM[3], AND DIEU TIEN BUI[4]

[1]Institute of Marine Geology and Geophysics, Vietnam Academy of Science and Technology, Cau Giay, Hanoi 10072, Vietnam
[2]Faculty of Earth Sciences, Graduate University of Science and Technology, Vietnam Academy of Science and Technology, Cau Giay, Hanoi 10072, Vietnam
[3]Center for Agricultural Meteorology, Vietnam Institute of Meteorology, Hydrology and Climate Change, Dong Da, Hanoi 10057, Vietnam
[4]GIS Group, Department of Business and IT, University of South-Eastern Norway, 3800 Bø i Telemark, Norway

Corresponding authors: Tran Anh Tuan (tatuan@imgg.vast.vn) and Dieu Tien Bui (Dieu.T.Bui@usn.no)

This work was supported in part by the Vietnam Academy of Science and Technology (VAST) under Grant VAST05.03/21-22; and in part by the Department of Business and IT, University of South-Eastern Norway, Bø i Telemark.

ABSTRACT Landslides are a significant geological hazard that annually cause extensive damage and loss of life worldwide. Therefore, it is crucial to have reliable prediction models for landslide susceptibility in order to identify high-risk areas and implement proactive measures to prevent or mitigate their impacts. The purpose of this study is to propose and evaluate a novel approach called BCMO-DeepNeuralNets for spatial prediction of the areas most susceptible to landslides. The study focuses on a tropical cyclone area in three districts of central Vietnam, namely Nam Tra My, Bac Tra My, and Phuoc Son. Accordingly, ten input factors were considered: slope, aspect, elevation, relief amplitude, land use, soil type, road distance, geology, fault distance, and rainfall. The proposed BCMO-DeepNeuralNets method leverages the power of Deep Neural Networks (DNNs) to develop a deep-learning model capable of inferring landslide susceptibility indices. To optimize this model, the study employs the Balancing Composite Motions Optimization (BCMO) technique. Additionally, Logistic Regression (LR) and Support Vector Machines (SVM) are used as benchmark models to confirm the efficacy of the proposed approach. To evaluate the prediction performance of the models, popular metrics such as mean squared error (MSE), accuracy (Acc), and Area Under the ROC Curve (AUC) are employed. The results show that the BCMO-DeepNeuralNets model exhibits high prediction performance, with an MSE of 0.038, Acc of 93.4%, and AUC of 0.971. This model outperforms the benchmark models, LR and SVM. Consequently, BCMO-DeepNeuralNets emerges as a new tool with significant potential for landslide susceptibility mapping. The landslide susceptibility map generated by this research aids in the identification of landslide-prone areas, providing a more accurate understanding of associated risks. As a result, it can be instrumental in policy and decision-making processes, enabling the implementation of appropriate measures to mitigate the impact of landslides in the study area.

INDEX TERMS Landslide, balancing composite motion, deep neural network, GIS, Vietnam.

I. INTRODUCTION

Landslides have considered one of the prevalent types of natural disasters that have significant direct and indirect impacts on society, the economy, and individuals [1], [2], [3]. Landslides have both direct and indirect consequences. The direct impacts include loss of life and injuries, destruction of buildings and infrastructure, as well as damage to natural resources and the environment. On the other hand, indirect impacts include economic losses due to the disruption of transportation and logistics services, expenses incurred from property relocation and resettlement, and environmental challenges that arise after disasters [4], [5].

The associate editor coordinating the review of this manuscript and approving it for publication was Gerardo Di Martino.

This work is licensed under a Creative Commons Attribution-NonCommercial-NoDerivatives 4.0 License.
For more information, see https://creativecommons.org/licenses/by-nc-nd/4.0/

Literature review shows that landslide susceptibility assessments can be separated into three groups: qualitative, semi-quantitative, and quantitative [6]. Qualitative and semi-quantitative methods are suitable for mapping at medium scale (1:250,000-1:25,000) and small scale (<1:250,000) [7]. These methods produce results often influenced by subjectivity and depend on expert experience. Representatives of these methods include inventory analysis, geomorphological mapping [8], [9], and multicriteria analysis [10], [11]. Meanwhile, the quantitative methods are suitable for mapping at large scales (1:25,000-1:5000) and detail scales (>1:5000) [7]. The commonly used quantitative methods are deterministic, probabilistic, statistical, and machine-learning approaches. Extensive reviews of the deterministic and probabilistic methods can be found in Grelle et al. [12] and Canli et al. [13], whereas a summary of statistical and machine-learning approaches can refer to [14], [15], and [16].

The recent development of artificial intelligence has resulted in various advanced machine learning and deep learning algorithms available in many open-source platforms, such as Python Weka API [17], Weka Deep Learning for Java [18], Google Tensor Flow [19], Keras deep learning [20]. As a result, the application of machine learning (ML) and deep learning (DL) in the spatial prediction of natural disasters has become increasingly popular, i.e., artificial neural networks [21], [22], [23], Support Vector Machines [24], [25], [26], [27], Decision Trees [28], [29], Random Forests [30], [31], Convolutional Neural Networks [32], [33], and Deep Neural Networks [34], [35]. In generall, deep learning has proven their efficient in landslide modeling and prediction compared to other ML algorithms [36], [37], [38], [39].

More recently, integrated models that combies two or more algorithms have gained popularity in landslide modeling [40], [41], [42] because they are capable of offering a more holistic and comprehensive approach to understanding landslide processes and improving prediction accuracy [43]. However, there has been limited research conducted on the investigation of integrated models that combine deep learning with optimization algorithms for landslide susceptibility modeling. Deep learning is particularly attractive in landslide modeling because it can effectively process large amounts of complex data, capture intricate relationships between landslide variables, automate feature learning, and enhance prediction power. On the other hand, optimization algorithms offer the ability to autonomously optimize the model, further improving the predictive capabilities of landslide models. Therefore, the integration of deep learning and optimization algorithms has the potential to significantly enhance the prediction power of landslide models.

This study aims to partially fill this gap in the literature by proposing a new landslide susceptibility mapping approach, namely BCMO-DeepNeuralNets, which combines the Balancing Composite Motion Optimization (BCMO) and deep neural network DeepNeuralNets). Herein, the DeepNeuralNets is used to generate a landslide model, whereas the BCMO, which is a relatively new machine learning optimization algorithm [44], is adopted to search and optimize the model parameters. The case study focuses on a tropical cyclone area located in central Vietnam in three districts, Nam Tra My, Bac Tra My, and Phuoc Son, which belong to the Quang Nam province. This province is situated in one of the areas with the highest rainfall levels in Vietnam and experiences frequent tropical cyclones. Consequently, landslides have become a significant issue in these districts, particularly over the past five years. For example, in 2017 alone, natural calamities triggered by heavy rainfall led to 37 fatalities and missing persons, with a total estimated cost of damages amounting to 70 million USD. Furthermore, the flood and landslide disasters that occurred in 2020 resulted in 43 deaths and 17 missing persons. Hence, there is an urgent need for research on landslides.

II. BACKGROUND OF THE EMPLOYED ALGORITHMS

A. DEEP NEURAL NETWORKS

In recent years, deep learning (DL), which is an advanced branch of machine learning, has become a hot research topic due to its ability to provide higher prediction capabilities in various spatial domains, i.e., forest fires [45], urban flood [46], flash flood [47], and landslides [48]. Basically, a deep neural network (DNN) is a feedforward artificial neural network consisting of multiple layers of interconnected nodes, also known as neurons. The feedforward means the data flow is unidirectional, moving solely from input to output [49]. Each layer performs a specific operation on the input data and passes the output to the next layer. First, the input layer of DNN receives the input data, then passes them to the first hidden layer. In the next step, each hidden layer performs a series of mathematical operations on the input data to compute the weights and biases of the network. Finally, the output of the final hidden layer is then passed to the output layer, which generates the final output of DNN.

Overall, the performance of DNN for spatial modeling is influenced by its structure and architecture. Therein, the number of hidden layers and neurons can vary depending on the complexity of the data and the training samples used. Nevertheless, the use of DNN is challenged by a prohibitively large number of weights and biased parameters, and how these parameters are updated and optimized in spatial domain applications are essential issues that should be addressed.

B. BALANCING COMPOSITE MOTION OPTIMIZATION

Balancing composite motion optimization (BCMO) is a meta-heuristic optimization algorithm introduced by. Le-Duc et al. [44]. BCMO stands out from other meta-heuristic algorithms due to its unique ability to perform both global and local searches within a defined search space. This characteristic ensures a balanced approach to solving various optimization problems. Thus, by utilizing this approach,

BCMO can tackle a broader range of optimization problems compared to other meta-heuristic algorithms [50].

The working mechanism of BCMO can be summarized below:

(1) Determine a searching space, population, and objective function for BCMO. Then, the distribution of the individuals is initialized and placed using the following equation.

$$x_i = LB_i + \text{rand}\,(1,D) \times (UB_i - LB_i) \quad (1)$$

$x_i = UB_i$ and LB_i are the position, the upper bound and the lower bound of the i^{th} individual in the defined searching space. $D \in [0,1]$ is the dimension of the searching space.

(2) Compute the score value for all individuals using the defined objective function and rank them to find the best individual.

(3) For each iteration (it), update the position of the i^{th} individual using Eq.2 and compute a new score value using the defined objective function.

$$x_i^{it+1} = x_i^{it} + v_{i/j} + v_j \quad (2)$$

where $v_{i/j}$ is the relative movement of the i^{th} individual concerning the j^{th} individual, v_j is the movement vector of the j^{th} individual.

(4) Repeat steps 2 and 3 until the termination condition is satisfied and the best position is found.

III. STUDY AREA AND LANDSLIDE DATA

A. DESCRIPTION OF THE STUDY AREA

The study area is located in the southwest of Quang Nam province, Vietnam, comprising three mountainous districts: Bac Tra My, Nam Tra My, and Phuoc Son. The site is situated in the Annamite Range in central Vietnam, between longitudes 107°38' and 108°30' E, and latitudes 14°56' and 15°35'N (see FIGURE 1).

Geologically, the study area is situated on the northern margin of the Indosini block, which is known for its complex geological structure and highly active fault zones. The region is dominated by metamorphic formations that occupy most of the area, while smaller areas contain intrusive magma formations with a variety of mineral compositions. The study area shares borders with various structural blocks, which have contributed to the formation of significant fault systems in the sub-latitude and sub-longitude directions. The sub-latitude fault systems include the Tam Ky - Phuoc Son fault system to the north and the Hung Nhuong - Ta Vi fault system in the center of the study area. The Po Ko River fault system, which runs in the sub-longitude direction, is located on the western margin.

It is important to note that the Tam Ky - Phuoc Son fault is considered an earthquake genetic region with an estimated maximum earthquake magnitude $_{\text{Mmax}} = 5.2$ [51]. The above fault systems are large tectonic fracture zones that significantly influence landslide events. Besides, the northwest-southeast fault system is well developed, creating diverse tectonic destructive scenery in the region.

The study area is a highly mountainous region with steep slopes, a dense network of streams, and intense dissection. The high mountains are distributed in the southwest and lower towards the northeast. The region includes several large mountain ranges, with high peaks exceeding 2000 m, such as Lum Heo (2045 m), Tion (2032 m), and Ngoc Linh (2598 m), which is the highest peak of the Annamite Range. The lowest elevation in the area is 20 meters above sea level. The primary soil type in the study area is Haplic Acrisol, accounting for 81.46% of the land.

The vegetation cover in the study area is typical of mountainous regions, accounting for 83.5% of the total area. The forest types include Protected forest, Productive forest, and Special-use forest. The climate is typical of the tropical region, influenced by the cold winter in the North of Vietnam, with two distinct seasons: the rainy and dry seasons. The rainy season usually lasts from September to December, while the dry season lasts from January to August annually. The study area belongs to one of the highest rainfall centers in Vietnam, and rainfall is concentrated during the four months of the rainy season. The average annual rainfall observed at Tra My station is over 4,000mm.

Economic activities are also rapidly developing, particularly with regard to the construction of road networks and hydropower dams in the catchments of the Vu Gia - Thu Bon rivers. These include Dak Mi 2, Dak Mi 3, Dak Mi 4A, B, and C, as well as Song Tranh 2, 3, and 4, and the Ta Vi reservoirs. However, the recent expansion of infrastructure and residential areas has led to rapid land use and forest cover changes, exacerbating the situation. In particular, the rudimentary and backward cultivation practices of local ethnic minorities, such as slash-and-burn farming and cultivation on steep slopes, have hurt nature. These economic developments have significantly reduced the upstream forest area and have increased the frequency and intensity of natural disasters such as landslides, flash floods, and mudflows.

The results of our fieldwork indicate that heavy rain periods, particularly the landfall of storm No. 9 (Hurricane Molave) in central Vietnam, intensified landslides and flash floods in late October and early November 2020. In addition, many of our survey sites showed evidence of devastated forests, with big trees drifting downstream due to natural disasters. Overall, both natural conditions and socio-economic development activities have significantly impacted the occurrence of natural disasters, particularly landslides, flash floods, and debris flows. During and after each prolonged heavy rain, large-scale landslides caused significant damage to people and property in the study area.

B. HISTORICAL LANDSLIDE LOCATIONS

The landslide inventory data in this study was collected to objectively identify the spatial distribution of past landslide events and as input data for the spatial prediction modeling of landslides. Therefore, this data did not show the

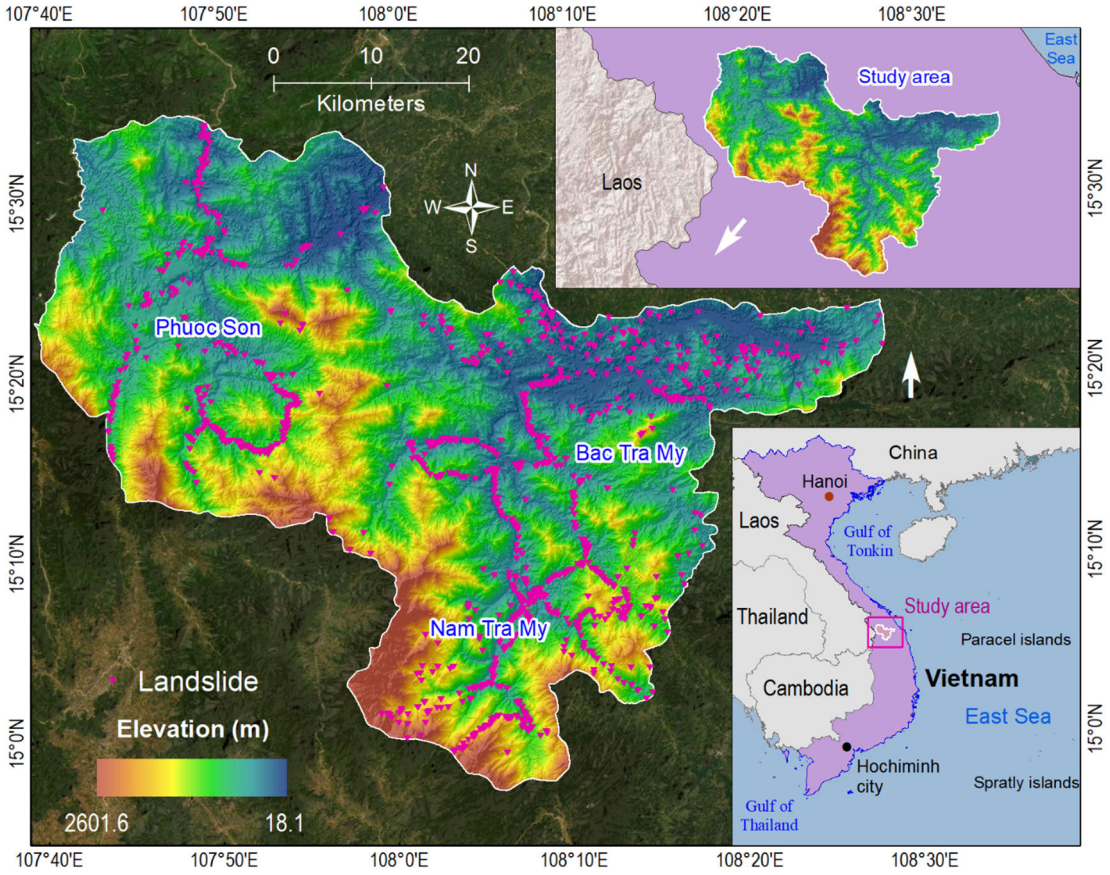

FIGURE 1. Location of the three districts (Nam Tra My, Bac Tra My, and Phuoc Son) and landslide locations.

scale, magnitude, and time of landslide occurrence. A total of 1698 landslide locations were identified from various sources. Firstly, the field survey collected data on 414 landslide sites, most of which were new and happened during the rainy season of October-November 2020. Secondly, 250 landslides in high-elevation areas were identified using Google Earth imagery due to difficulties accessing these areas during fieldwork. In addition, we included 495 landslide points from previous studies in Vietnam, of which 220 were found along the road system. These data were obtained from the Ministry of Science and Technology National project on ''Landslide hazard prediction along the mountainous transport arteries in Quang Nam province and the adaptation measures [53]'', which can be accessed at http://quangnam.truotlo.com.

Finally, 59 landslides were from the State-Funded Landslide Project (SFLP), namely ''Investigation, assessment and warning zonation for landslides in the mountainous regions of Vietnam'' [52; 21 landslides get from the national research project: ''To study, supplement and develop a map of natural disasters in Vietnam's mainland based on research results from 2000 up to now'' [53; and 95 landslides were from the project of the Vietnam Academy of Science and Technology on ''Landslide hazard assessment by geological and geomorphological methods integrated with the GIS optimal weighting model in river basins in Thua Thien Hue, Quang Nam, and Da Nang areas, proposing solutions prevent'' [54].

The survey results on landslide status in the study area show that most landslides occurred in the weathered crust with various block sizes. After prolonged heavy rains, many arterial roads, such as national highways 14G, 40B, 14E, and Ho Chi Minh roads through the area, often suffered landslides causing traffic to be discontinuous. Severely, landslides also cause death and bury houses due to the custom of building residences on high mountain slopes of ethnic minorities. For example, the prolonged rain in early November 2017 caused landslides occurrence widely in the mountainous area of Quang Nam province. Notably, the landslide that killed five people occurred in Tra My town, Bac Tra My district, on 5 November 2017. On the same day, a landslide that lost two people occurred in Phuoc Hoa commune, Phuoc Son district.

During the rainy season lasting from late October to early November 2020, some typical landslides with severe consequences occurred as follows: The landslide that buried 15 houses, including 09 dead, 13 missing, and 33 people injured, occurred in Ong De residential cluster, Tra Leng Commune, Nam Tra My district on 28 October 2020. The landslide position was at the small stream that flowed into

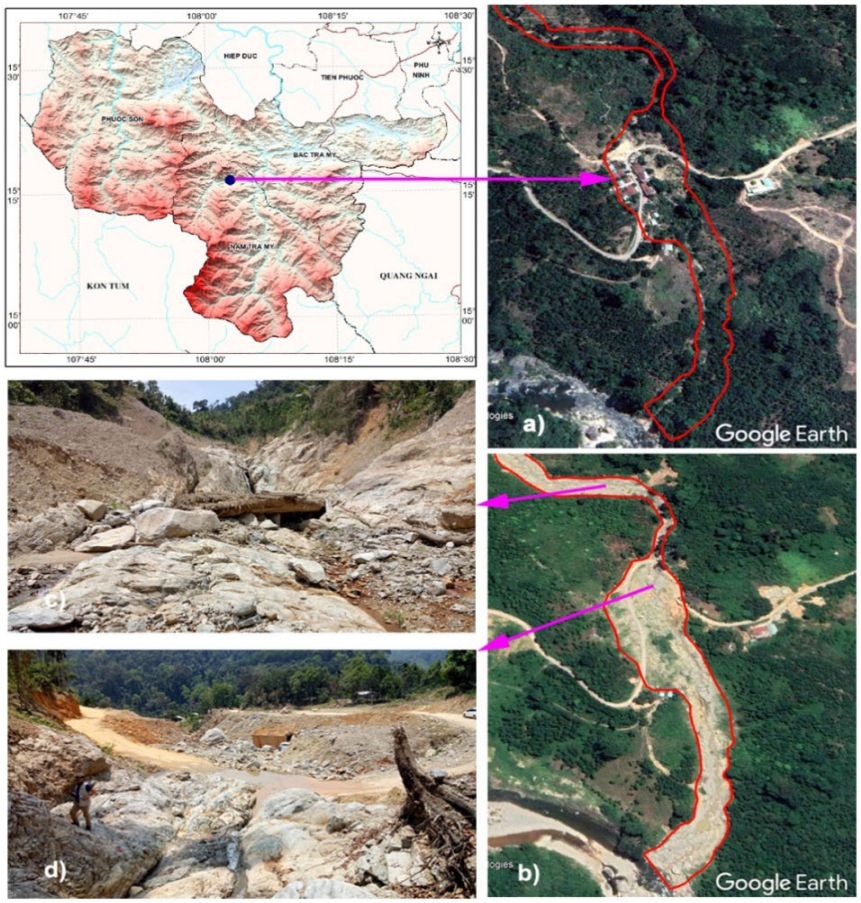

FIGURE 2. The landslide area at Ong De residential cluster, Village 1, Tra Leng commune, Nam Tra My district, Quang Nam province on 28 October 2020: a) The scene before the landslide occurred (Google Earth image at April 2019; b) The scene after the landslide occurred (Google Earth image at June 2021); The location of the landslide body where the weathering crust was removed exposing the bedroc; and d) The location of the landslide where the material of the landslide buried 15 houses, 09 deads, 13 missings, and 33 people injured. Photographs were taken on April 2021 by Tran Anh Tuan and Phan Dong Pha.

the mainstream. The lithology of the landslide area is Gneiss, with foliation, puckering, metamorphism, and developing a dense fracture system (FIGURE 2), a landslide severely damaged a road that occurred in Tra Mai commune, Nam Tra My district. This landslide occurred in the weathered crust of the Tac Po formation, composed of micro-folded schist in Migmatite form (see Figure 3a). On the same day, another landslide buried three houses and caused eight deaths in Hamlet 1, Tra Van commune, Nam Tra My district. The landslide is a large mass with dimensions of width, length, and height of 45 m, 60m, and 15 m, respectively, steep slope of about 40°. The sliding surface coincides with the foliated surface of the bedrock. The weathered crust is thick and consists mainly of silty sand of the Tac Po Formation. Although the vegetation is a well-planted forest, prolonged heavy rains make the soil saturated with water causing landslides (FIGURE 3b); The landslide caused a whole village to be displaced, and two commune officials were lost while helping people in landslide areas of Phuoc Loc commune, Phuoc Son district. The landslide occurred in the weathered crust of the Kham Duc Formation with medium natural forest (FIGURE 3c).

C. LANDSLIDE-RELATED FACTOR

Landslide-related factors are natural and human factors that directly or indirectly trigger landslide occurrence, including geological conditions, geomorphological features, rainfall, land use and land cover, and human development activities [55]. We selected ten landslide-related factors as input parameters for the landslide prediction model based on their spatial differentiation in the study area. These factors include elevation, relief amplitude, slope, aspect, geology, soil type, distance to roads, distance to faults, land use, and rainfall.

Firstly, national topographic maps at a scale of 1:50,000 were collected and merged to generate a digital elevation model (DEM) with a spatial resolution of 20 m. Next, four geomorphometric factors: elevation, relief amplitude, slope, and aspect, were extracted from the DEM. These factors were classified using the Natural Break method to ensure

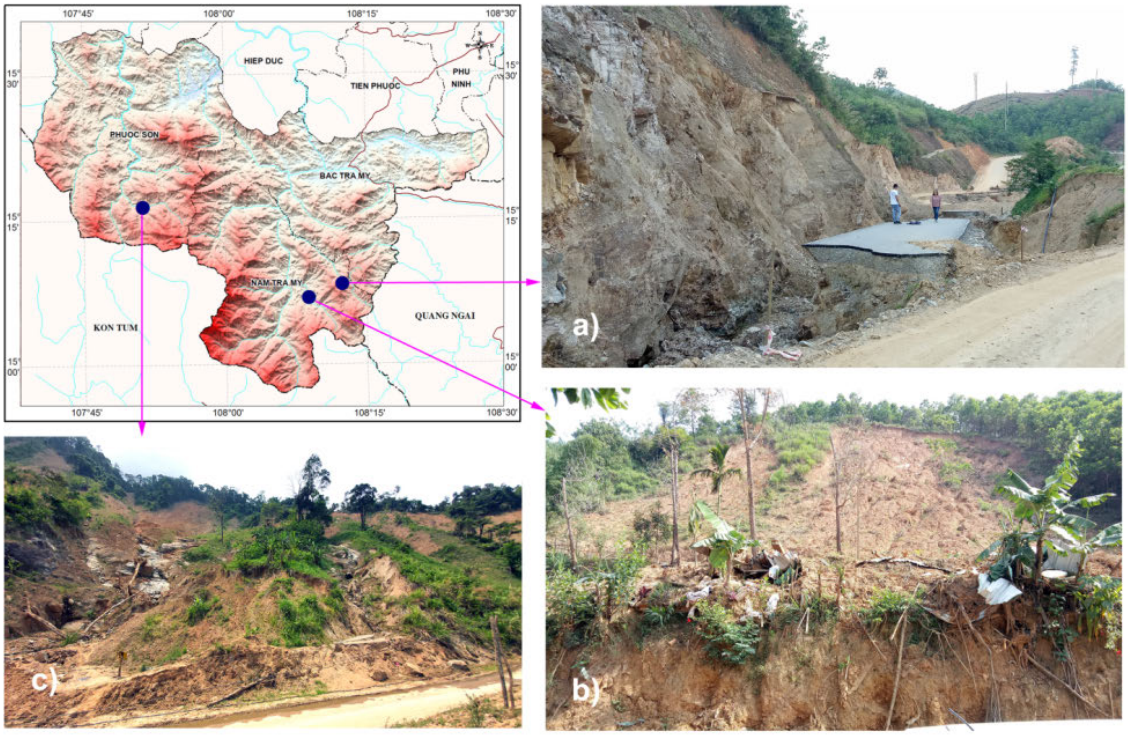

FIGURE 3. Some typical landslides in the study area had occurred on 28 October 2020: a) Landslide at Tra Mai Commune, Nam Tra My District destroyed a road section; b) landslide in Tra Van commune, NamTra My district buried three households with a total of eight deaths; and c) landslide in Phuoc Loc commune, Phuoc Son district, causing loss of two people. Photographs were taken on April 2021 by Tran Anh Tuan and Phan Dong Pha.

objectivity and their spatial distribution characteristics. As a result, the elevation (FIGURE 4a) was constructed with ten classes. Nine classes were used for the relief amplitude, slope, and aspect (FIGURE. 4b, 4c, and 4d).

We extracted two geological factors, namely, stratigraphy with various lithological features and distance to faults, from the 1997 Geological and Mineral Resources maps published on a 1:200,000 scale by the General Department of Geology and Minerals of Vietnam. The geological map shows mainly metamorphic rock formations consisting of the Tac Po (PR_1 tp), Song Re (PR_1sr), Kham Duc ($PR_{2-3} - \in_1 kd$), A Vuong ($\in_2 - O_1 av$), Dak Long ($\in - Sdlg$) formations, and small distributions of Dai Nga Formation ($\beta N_2 dn$) and Undivided Quaternary (edQ). Intrusive magma complexes distribute in small areas with quite diverse mineral compositions, including the main complexes such as TaVi ($PR_3 tv$), Chu Lai ($PR_3 cl$), Tra Bong (O-S tb), Ben Giang - Que Son (PZ $bg - qs$; Deo Ca(Kdc), BaNa(K $-$ Ebn) complexes, and other complexes have limited distribution area (FIGURE 4e). The distance to faults map was constructed with five classes based on buffering polylines of faults (FIGURE 4h).

The soil type factor was extracted from the soil type map of Quang Nam province at a 1:50,000 scale, which used the FAO-UNESCO soil classification system. The soil type map of this study was constructed with fourteen classes by grouping similar Soil Subunits (FIGURE 4f).

The result of the field survey showed that landslides occurred on roads in the 2020 rainy season. The construction of traffic works in the study area has significantly impacted the stabilization of slopes leading to landslides that have occurred in the water-saturated soil layers by prolonged and heavy rains on both negative and positive slopes of the roads. Therefore, the distance to road factor that was extracted from the topographic map at a 1:50,000 scale was selected and constructed with six classes based on buffering polylines of roads (FIGURE 4g). However, parts of the road system were eliminated from slope areas that were less than five degrees in this study.

The land use map of the study area includes eight land-use types (FIGURE 4i). Two forest types with the largest total areas are productive and protected forests. Their area percentages are approximately 37.45% and 35.28%, respectively. The land use types with relatively large areas are special-use forests (10.76%) and perennial crops (9.60%). The remaining land use types that occupy the little area are annual crops (2.62%), rice land (1.79%), water surface (1.53%), and residential land (0.97 %). The land use factor was extracted from the land use map of Quang Nam province in 2015 at a 1:50,000 scale.

The rainfall map presents the total highest rainfall in three months of the rainy season from September to November 2020, which was the time when landslides occurred most

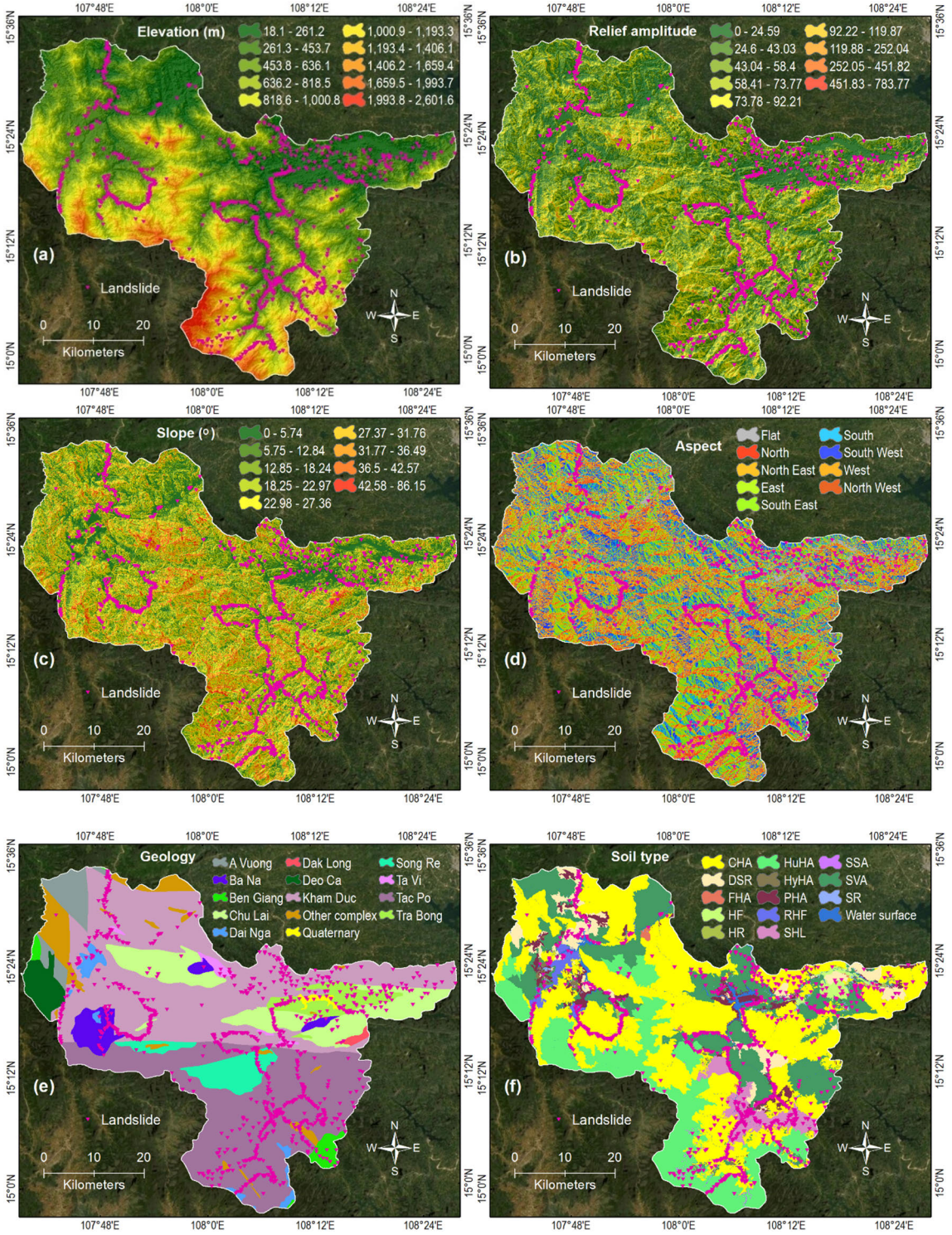

FIGURE 4. Landslide influencing factors: (a) Elevation (m); (b) Relief amplitude; (c) Slope (°); (d) Aspect; (e) Geology; and (f) Soil type. PHA: Profondi- Haplic Acrisol; SVA: Skeleti- Vetic Acrisol; SSA: Skeleti- Stagnic Acrisol; CHA: Chromi- Haplic Acrisol; HuHA: Humi- Haplic Acrisol; HyHA: Hyperdystri- Haplic Acrisoll; HF: Haplic Fluvisol; SHL: Skeleti- Haplic Leptosol; RHF:Rhodic- Haplic-Ferrasols; HR: Haplic Regosol; SR: Stagnic Regosol; DSR: Dystri- Stagnic Regosoll; FHA: Ferri- Haplic Acrisol. (g) Distance to road (m); (h) Distance to fault (m); (i) Landuse; and (j) rainfall (mm).

commonly in the study area. The rainfall map was subsetted by the study area boundary from the grid data that had interpolated using the Inverse Distance Weighed method; then, it was classified into seven classes using the Natural Break method (FIGURE 4j). The precipitation data were continuously collected from 27 rain gauges, of which two stations

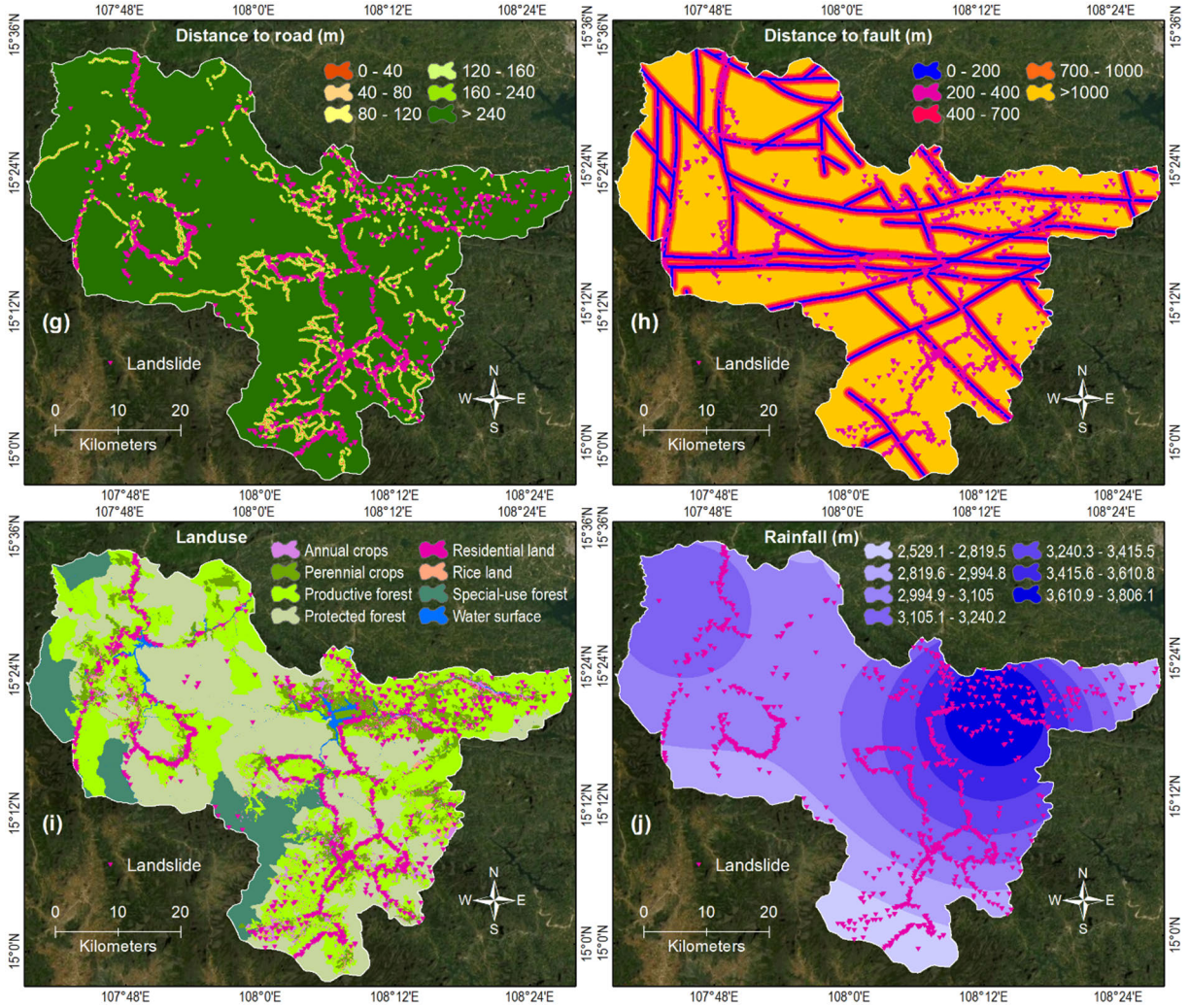

FIGURE 4. *(Continued.)* **Landslide influencing factors: (a) Elevation (m); (b) Relief amplitude; (c) Slope (°); (d) Aspect; (e) Geology; and (f) Soil type. PHA: Profondi- Haplic Acrisol; SVA: Skeleti- Vetic Acrisol; SSA: Skeleti- Stagnic Acrisol; CHA: Chromi- Haplic Acrisol; HuHA: Humi-Haplic Acrisol; HyHA: Hyperdystri- Haplic Acrisoll; HF: Haplic Fluvisol; SHL: Skeleti- Haplic Leptosol; RHF:Rhodic- Haplic- Ferrasols; HR: Haplic Regosol; SR: Stagnic Regosol; DSR: Dystri- Stagnic Regosoll; FHA: Ferri- Haplic Acrisol. (g) Distance to road (m); (h) Distance to fault (m); (i) Landuse; and (j) rainfall (mm).**

were located in the study area. These data were sourced from the Vietnam Institute of Meteorology, Hydrology and Climate Change.

IV. PROPOSED METHODOLOGY FOR SPATIAL PREDICTION OF LANDSLIDE

The flowchart of the proposed BCMO-DeepNeuralNets model for spatial prediction of landslides is shown in FIGURE 5. In this project, ArcGIS Pro 2.9.5 was used to manage and process the inventory map and the landslide-related factors. The Matlab code of the BCMO algorithm can be found in..Le-Duc, et al. [44], while the BCMO-DeepNeuralNets model was written by the authors using the Deep Learning Toolbox in the Matlab R2019b. In addition, a Python script was also developed by the authors to transfer the susceptibility indices derived from the BCMO-DeepNeuralNets model into ESRI geodatabase format for cartographic presentation of the final landslide susceptibility map

A. STEP 1—DATABASE ESTABLISHMENT

First, a GIS database is established using the ESRI file geodatabase format [56] in ArcGIS Pro. This geodatabase format is selected because it is stored and organizes landslide data in a system folder that is optimized for storage and performance, improving usability in the modeling process. The database consists of 1698 landslide locations and ten landslide-related factors (elevation, relief amplitude, slope, aspect, geology, soil type, distance to road, distance to fault, landuse, and rainfall). Herein, all factors were converted into a raster format with a grid cell of 20 m.

Landslide modeling with deep neural networks required data samples to be in the range of 0 and 1; therefore, a spatial rescaling process was carried out to normalize all raster

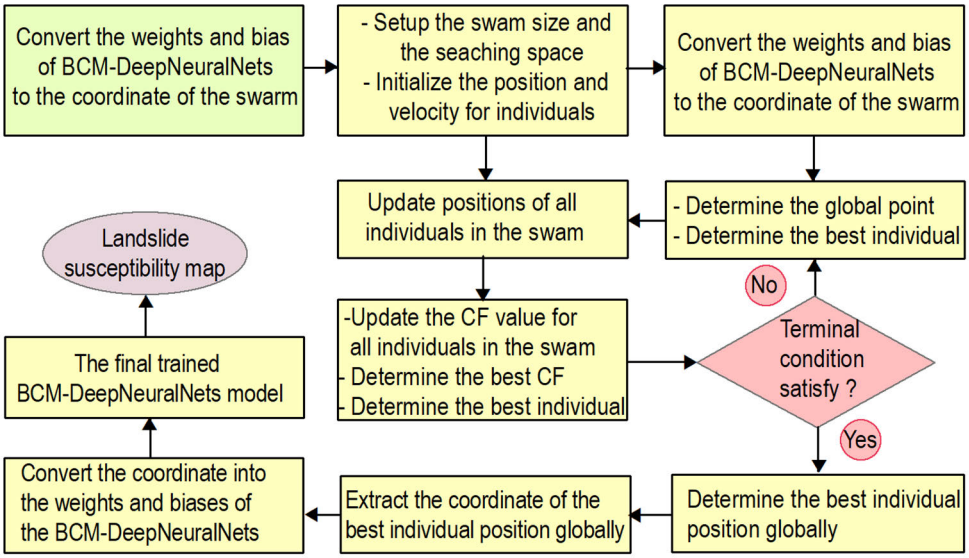

FIGURE 5. Flowchart of the BCM algorithm for optimizing the Deep-NeuralNets model.

values of the ten landslide related factors in a range of 0.01 to 0.99 in ArcGIS Pro using Eq.1 below:

$$LF_j = \frac{LF - Min(LF)}{Max\,(LF) - Min(LF)} * 0.98 + 0.01 \tag{3}$$

where LF_j and LF are the new raster value and original raster value of landslide-related factors (LF). $Max\,(LF)$ and $Min(LF)$ are the maximum and the minimum values of the landslide-related factors.

For landslide modeling, among 1698 landslide locations, a total of 1189 locations (70%) were randomly sampled and used for training landslide models, whereas the remaining 509 locations (30%) were used for validating the modeling results. In addition, the same amount of non-landslide locations [57] were randomly created for the study area. Finally, we sample values of the ten landslide-related factors for both landslide and non-landslide locations using the sampling tool in ArcGIS Pro.

B. STEP 2–SELECTION OF OBJECTIVE FUNCTION

As mentioned in section II-B, in order to determine the best solution with the BCMO, an objective function must be defined. In this work, we select the Mean Squared Error (MSE) for the objective function as below:

$$MSE = \frac{1}{n}\sum_{i=1}^{n}(T_i - O_i)^2 \tag{4}$$

where T_i is the target value of the landslide data; o_i is output value from the model; n is the number of samples.

C. STEP 3–FEATURE SELECTION

As mentioned above, ten landslide-related factors are qualitatively selected based on landslide mechanism analysis and the geo-environmental characteristics of the study area. However, to ensure all the factors are relevant or not redundant, the worth of the landslide-related factors is further checked using the Wrapper-based Random Forest (WRS) technique [58] and the 5-fold cross-validation technique. Herein, a forest of 500 random trees was employed to search for possible combinations of the landslide-related factors. Then, the evaluator of MSE (Eq.4 above) is used to assess the best subset, and finally, each factor's worth is ranked.

D. STEP 4–MODEL CONFIGURATION

In this research, we design the DeepNeuralNets model (FIGURE 6) for spatial prediction of landslide with ten neurons in the input layer (IL), 16 neurons in both the first hidden layer (H1) and the second hidden layer (H2), one neuron in the output (OP). Therefore, a total of 465 parameters were defined. A detailed explanation of these parameters relating to the weight and bias of the proposed model is shown in Table 1.

The goal of training the BCMO-DeepNeuralNets is to search and find the optimized values for the weight and bias of the model. Therefore, a searching space (D) of 465 dimensions was established (Eq.5). These parameters were organized into a matrix $1\times D$. The lower bound (LB) and the upper bound (UP) were selected as -1 and 1, respectively. The population of 85 individuals is selected, and the maximum iteration of 2000 is adopted.

$$\begin{aligned} D = {} & IW_{10\times 16} + NB1_{16} + HL1_{16\times 16} \\ & + Bias2_{16\times 1} + HL2_{1\times 16} + Bias3 \end{aligned} \tag{5}$$

In the searching space D, the coordinate of each individual in 465-dimensional space is obtained; thus, each position is a solution of the BCMO-DeepNeuralNets model. When an individual moves to a new position, a new solution is obtained and tested, and the optimization process is carried out to find the best position where MSE is minimum.

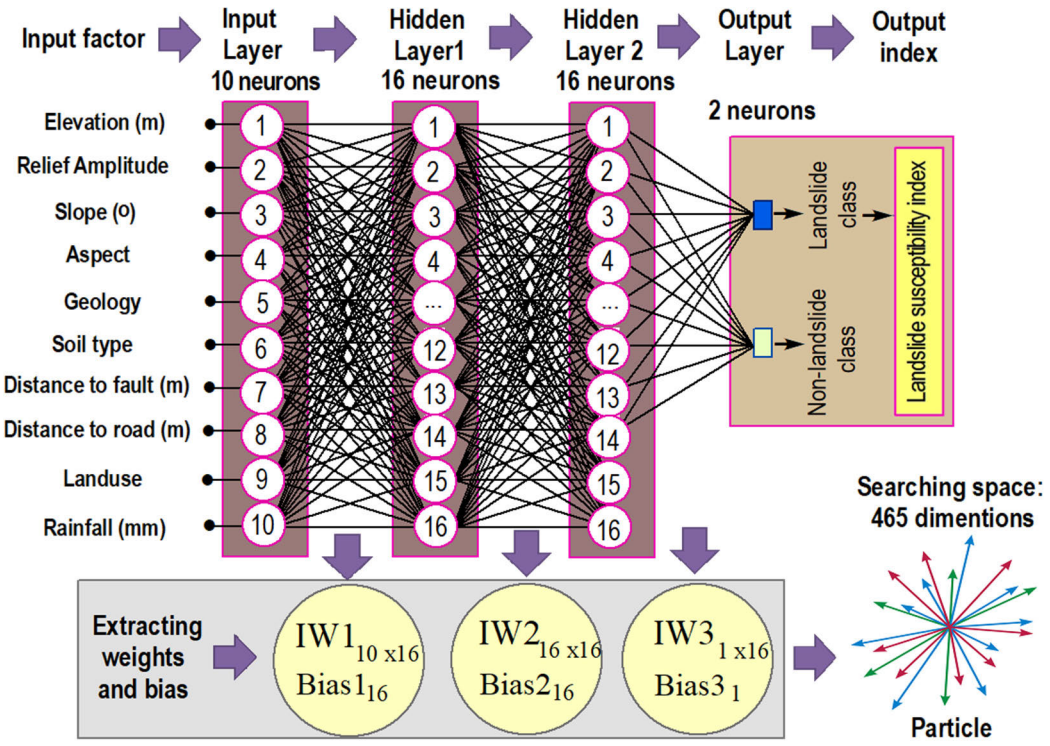

FIGURE 6. The proposed BCM-DeepNeuralNets model for spatial prediction of landslide in this research.

TABLE 1. Weight and bias of the DeepNeuralNets.

No	Name	Matrix	Parameter
1	Weight of the input layer	IW_{10x16}	160
2	Network Bias1	$Bias1_{16x1}$	16
3	Weight of the hidden layer1	$HL1_{16x16}$	256
4	Network Bias2	$Bias2_{16x1}$	16
5	Weight of the hidden layer2	$HL2_{1x16}$	16
6	Network Bias3	$Bias3_{1x1}$	1

E. STEP 5–PERFORMANCE EVALUATION

In order to assess the performance of the BCMO-DeepNeuralNets model, the mean squared error (MSE) (Eq.4), Accuracy (Acc), Receiver Operating Characteristic (ROC) curve, area Under the ROC Curve (AUC), Positive Predictive Value (PPV), Negative Predictive Value (NPV), and Kappa Coefficient (Kappa) were used. They are the most popular and widely accepted statistical metrics used in landslide modeling. Because these metrics have been overwhelmingly published in the literature, we do not repeat them here again, and readers can refer to papers, i.e.,. Tien Bui et al. [26] or Gorsevski [59].

V. RESULTS AND DISCUSSION

A. FEATURE SELECTION

The ranking result of the landslide-related factors using the WRS technique with the 5-fold cross-validation is shown in Table 2.

It could be seen that all factors offer merit values for landslide modeling; however, the worth of landslide-related factors is different. Herein, the slope and the distance to road provide the highest values, where the merit score is 0.338 and 0.171, respectively. They are followed by the landuse (0.123), the relief amplitude (0.095), the elevation (0.161), and the soil type (0.061). In contrast, the rainfall (0.016) and the distance to fault (0.009) contribute to the lowest merit scores (Table 2).

B. MODEL PERFORMANCE

Searching and optimizing the 465 parameters of the Deep-NeuralNets was performed using the MCMO algorithm with 2000 iterations used. The best individual position was found with $MSE = 0.038$. Then, the coordinates of the best individual in 465 dimensions were extracted, and the final weights and biases were obtained for the BCMO-DeepNeuralNets model. The training result of the proposed BCMO-DeepNeuralNets model presented in Table 3 shows

TABLE 2. Evaluating the worth of landslide-related factors using the WRS technique with the 5-fold cross-validation.

Landslide related factor	Merit score	Ranking
Slope	0.338	1
Distance to road	0.171	2
Landuse	0.123	3
Relief amplitude	0.095	4
Elevation	0.067	5
Soil type	0.061	6
Aspect	0.050	7
Geology	0.027	8
Rainfall	0.016	9
Distance to fault	0.009	10

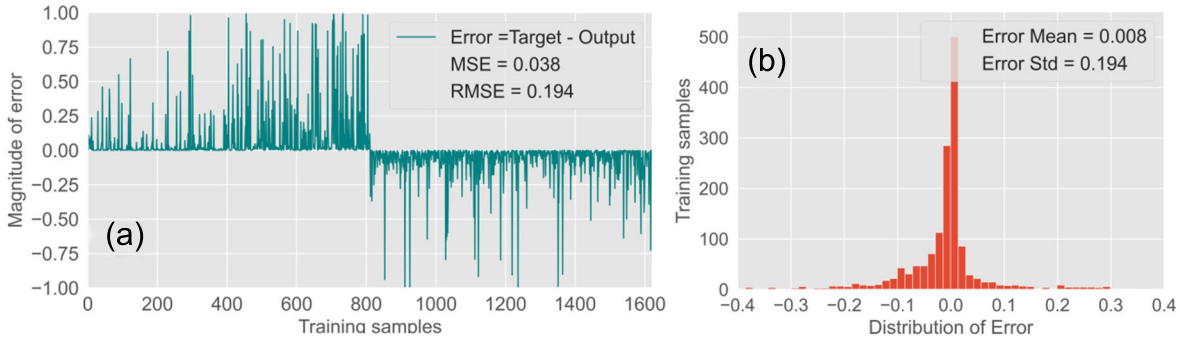

FIGURE 7. Performance of the BCMO-DeepNeuralNets model in the training dataset; (a) Magnitude of the errors and (b) Distribution of the error.

Acc = 95.7%, Kappa = 0.915, F-score = 0.957, and AUC = 0.983 demonstrating that the model yields a high degree of fit with the training data. Mean and standard (Std) errors are 0.008 and 0.194, respectively (FIGURE 7), indicating a low error was achieved. The other statistical metrics are shown in Table 3.

The validation result is shown in Table 4 and FIGURE 8. It can be seen that the proposed BCMO-DeepNeuralNets model (Acc = 95.7%, Kappa = 0.915, F-score = 0.957, AUC = 0.971) shows a high prediction power. The spread of errors of the BCMO-DeepNeuralNets model is narrow, with the mean error (0.008) and standard error (0.194) being small, suggesting that the model works well and is likely to produce reliable predictions with new landslide data.

The global performance of the proposed BCMO-DeepNeuralNets model measured by the ROC curve and AUC is shown in FIGURE 9. AUC of 0.971 in the validation dataset indicates that the model is making accurate landslide predictions with slight variation in the classification threshold. The good ROC curve also indicates that the model is not biased toward either landslide or non-landslide cases

C. MODEL COMPARISON

In order to ensure the effectiveness of the proposed BCMO-DeepNeuralNets model for landslide susceptibility modeling, it is essential to compare the prediction power of the model with those produced by baseline methods.

Herein, logistic regression (LR) and support vector machines (SVMachine) were selected as the baseline models due to their robustness with good performances in various works [27], [60]. For the SVMachine model, the Radial Basis Function (RBF) kernel function with C=9.8 and $\gamma = 0.05$ was used. The results in Tables 3 and 4 show that the LR and SVMachine models yielded high performance on both the training and the validating datasets, as indicated by Acc, F-score, Kappa, and AUC. However, their statistical matrices are lower than those of the proposed BCMO-DeepNeuralNets model.

To statistically verify that the performance of the proposed BCMO-DeepNeuralNets model surpassed that of the baseline models, a Wilcoxon test was further conducted. The hypothesis tested (Ho) is that the performance of the BCMO-DeepNeuralNets model is not significantly different from that of the baseline models. In order to assess this, the Z-value and p-value were calculated. The critical values of ± 1.96 were used to determine whether the calculated Z-value is significant at the 5% significance level. Suppose the calculated p-value is less than 0.05, and the Z-value exceeds these critical values. In that case, it is considered statistically significant and indicates that the performance of the BCMO-DeepNeuralNets model is better than that of the baseline models.

The result shown in Table 5 shows that the p-value is less than 0.05 and Z-value exceeds the critical values of ± 1.96,

TABLE 3. Performance of the BCMO-DeepNeuralNets model and the benchmark using the training dataset.

Model with 5-fold cross-validation	Statistical metrics											
	TP	TN	FP	FN	PPV	NPV	Sens	Spec	Acc	F-score	Kappa	AUC
BCMO-DeepNeuralNets	762	791	49	20	94.0	97.5	97.4	94.2	95.7	0.957	0.915	0.983
Logistic regression	601	679	210	132	74.1	83.7	82.0	76.4	78.9	0.778	0.578	0.889
SVMachine	626	693	185	118	77.2	85.5	84.1	78.9	81.3	0.805	0.626	0.908

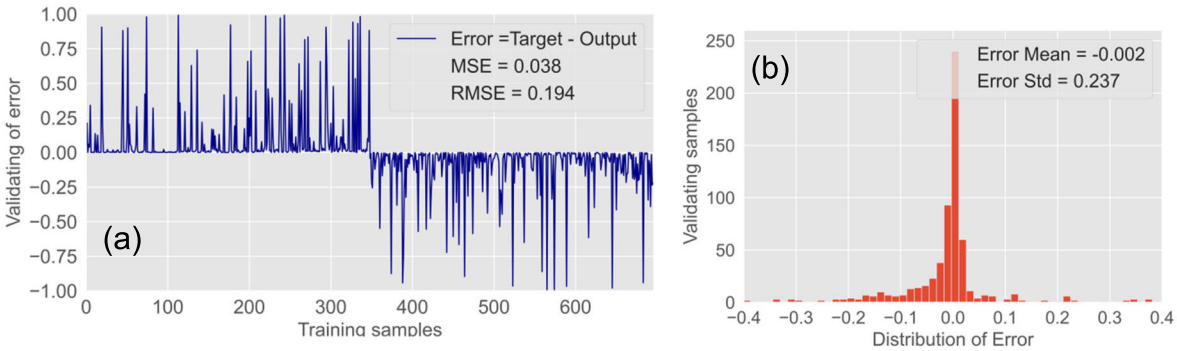

FIGURE 8. Performance of the BCMO-DeepNeuralNets model in the validating dataset; (a) magnitude of the errors and (b) error distribution.

TABLE 4. Performance of the BCMO-DeepNeuralNets model and the benchmark using the validating dataset.

Model with 5-fold cross-validation	Statistical metrics											
	TP	TN	FP	FN	PPV	NPV	Sens	Spec	Acc	F-score	Kappa	AUC
BCMO-DeepNeuralNets	323	327	25	21	92.8	94.0	93.9	92.9	93.4	0.934	0.868	0.971
LR	261	298	87	50	75.0	85.6	83.9	77.4	80.3	0.792	0.606	0.896
SVMachine	276	302	72	46	79.3	86.8	85.7	80.7	83.0	0.824	0.661	0.917

indicating that the BCMO-DeepNeuralNets model performs better than the LR model and the SVMachine model.

D. LANDSLIDE SUSCEPTIBILITY MAP

The final BCMO-DeepNeuralNets model was then used to compute the susceptibility indices for all pixels of the study area. Herein, the susceptibility values vary from 0.00 to 1.00. In the next step, these susceptibility indices were converted to a raster map with 3461 rows x 4362 columns using the Python script mentioned in Section IV. The susceptibility indices were cartographically presented in five susceptibility classes [61], very low (0.00-0.119), low (0.119.0.176), moderate (0.76-0.952), high (0.952-0.986), and very high (0.986-1.000) (FIGURE 10).

Thresholds for five susceptibility classes were determined using the method described by.Chung and Fabbri [62]. Accordingly, the landslide inventory map was crossed with the susceptibility index map, and then, the percentage of the landslide pixels versus the percentage of the landslide susceptibility map was determined. Subsequently, a graph

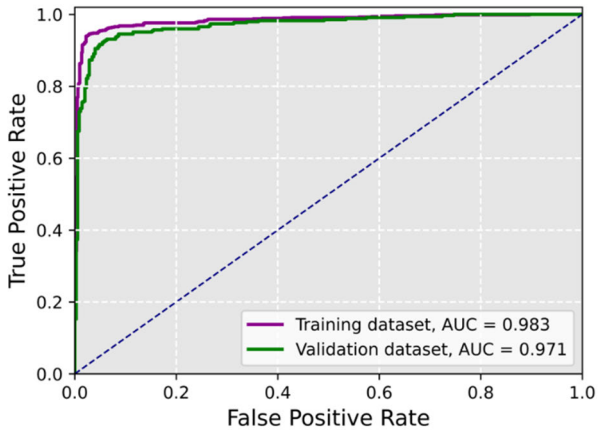

FIGURE 9. The ROC curve and AUC for the proposed BCMO-DeepNeuralNets model.

was generated (FIGURE 11), and the four thresholds were obtained as 0.986, 0.952, 0.760, and 0.119. Herein, 15% of the study area was used for the very high class, whereas the

TABLE 5. Wilcoxon test for the three landslide models.

No.	Pairwise comparison	Z-value	*p*-value	Statistical significance
1	BCMO-DeepNeuralNets - LR	2.133	0.033	Yes
2	BCMO-DeepNeuralNets - SVMachine	3.084	0.002	Yes

TABLE 6. Properties of the five susceptibility classes derived from the proposed BCMO-DeepNeuralNets.

No	Susceptibility index	Landslide pixel (%)	Susceptibility map (%)	Areas (km^2)	Description
1	0.986 -1.000	41.30	15.0	425.70	Very High
2	0.952-0.986	14.98	20.0	567.60	High
3	0.760-0.952	12.12	20.0	567.60	Moderate
4	0.119-0.760	10.74	20.0	567.60	Low
5	0.000-0.119	3.46	25.0	709.50	Very Low

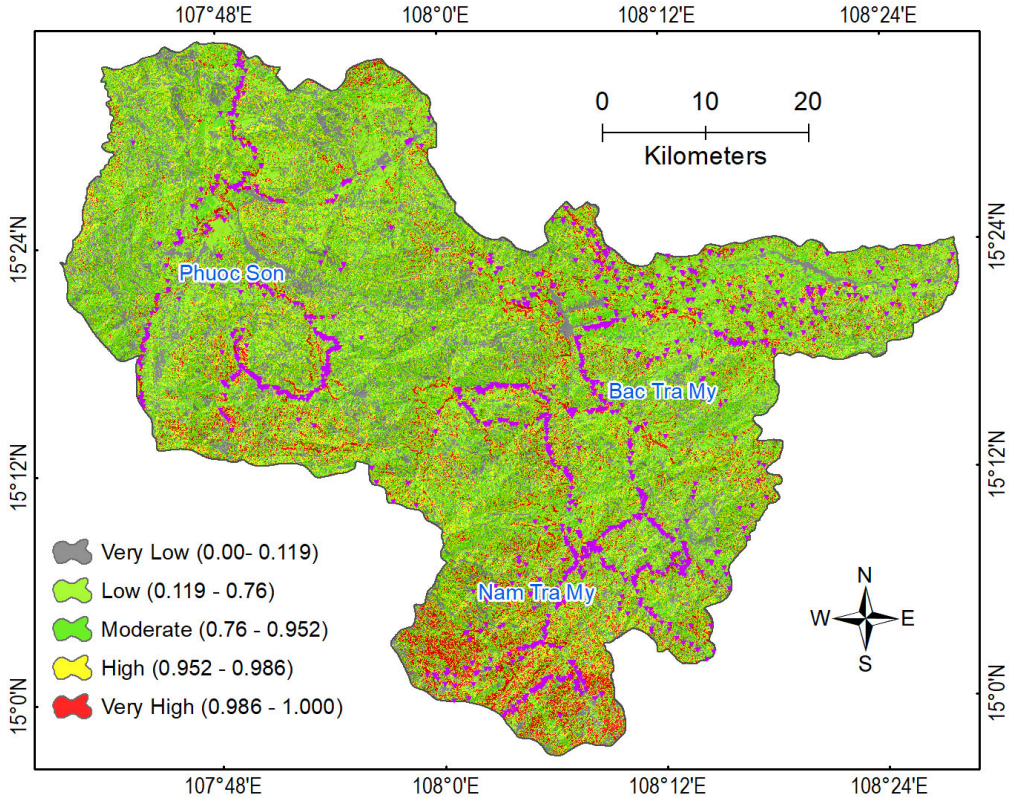

FIGURE 10. Landslide susceptibility map for the study area using the proposed BCM-DeepNeuralNets model.

very low class accounts for 25% of the study area, and 20% was used for each of the three classes, high, moderate, and low (FIGURE 11).

The properties of the five susceptibility classes are shown in Table 6. It could be seen that 41.30% of the landslide pixels are located in the very high class. This class accounts for 15.0% of the total study area, covering 425.70 km^2. In contrast, only 3.46% of the total landslide pixels are in the very low class, with 709.50 km^2 (Table 6). It denotes that the proposed BCMO-DeepNeuralNets is capable of highlighting landslide risk areas.

VI. DISCUSSION

Landslides are continuing as one of the significant causes of damage and fatalities across the globe. The economic impact of landslides is staggering, with billions of dollars in damages estimated to occur each year [63]. In addition, thousands of deaths each year due to landslides [64] pose a significant threat to human safety and well-being. Besides, climate change and improper land use planning in recent years somewhat exacerbate the problem. Therefore, it is essential to have reliable prediction models for landslide susceptibility, as they have a critical role in identifying landslide

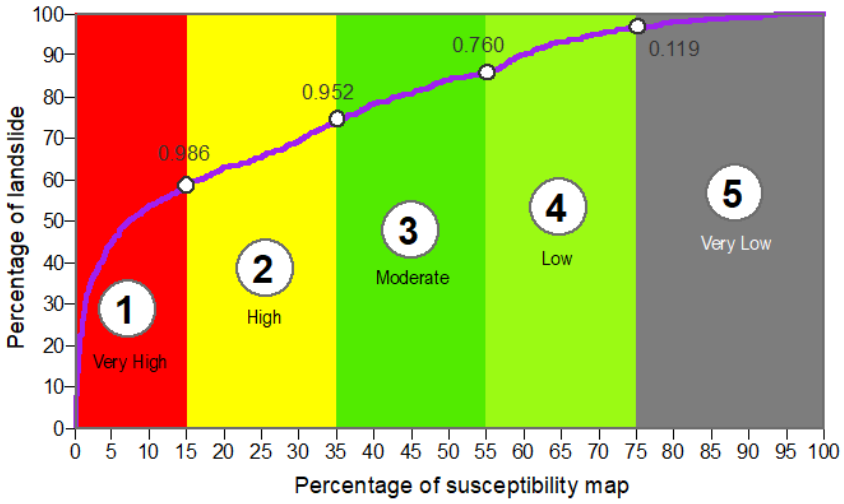

FIGURE 11. Graph for determining the four thresholds for the five susceptibility classes.

risk areas, allowing for proactive measures to be taken to prevent or mitigate their impacts. In this work, a new landslide susceptibility modeling approach has been developed and tested. This innovative approach involves employing DeepNeuralNets combined with BCMO, named BCMO-DeepNeuralNets, to generate predictions of where landslides are most likely to occur. Then, the BCMO-DeepNeuralNets model is tested at a recurring landslide area in central Vietnam. In this area, landslides have been severe in the last three years due to the continuous occurrence of hefty rainfall.

DeepNeuralNets with two hidden layers containing 32 neurons are used to generate a landslide model, whereas the BCMO algorithm trains and optimizes the model. The BCMO provides equalization in the search and optimization, helping the model training process achieve faster convergence. The high performance of the proposed model indicates that the BCMO successfully searched and optimized the weights of the DeepNeuralNets. The result of this research is in line with that of recent studies, where deep learning models with structurally diverse adaptive scaling have demonstrated high predictive power in many spatial domains [16], [65], [66].

Overall, the performance of the DeepNeuralNets model is still strongly dependent on its structure used. However, it is still not easy to design a deep learning model for landslide susceptibility modeling to determine how many hidden layers and how many neurons should be used for each layer. Although two hidden layers with 32 hidden neurons are used for the DeepNeuralNets model, there is no guarantee that this is the best structure for the data at hand. Thus, further research should be carried out regarding the autonomous determination of the deep learning structure. Nevertheless, the DeepNeuralNets model performs better than the benchmark, the LR model, and the SVMachine model, the combination of the BCMO and the DeepNeuralNets bring a new solution for landslide susceptibility mapping.

Identifying the critical factors contributing to landslide occurrence found that the ten factors considered, but three factors, slope, distance to roads, and land use, emerged as the most critical factors. It is a logical result since the slope is consistently the primary contributing factor for landslides [67], [68]. Distance to roads is another critical factor identified by the study because the construction of roads in the study area destabilizes slopes by removing vegetation, altering drainage patterns, and increasing surface water flow. Besides, changes in land use are another critical cause of landslides. It should be noted that the study area is located in Quang Nam province, where the economic growth rate has been high in recent years [69]. The development of infrastructure and the expansion of economic development types have significantly changed the nature of land use here [70], [71].

VII. CONCLUDING REMARKS

In this study, a new approach based on BCMO-DeepNeuralNets for landslide susceptibility mapping has been proposed and tested. This modeling approach incorporates ten geo-environmental factors contributing to landslide occurrences: slope, aspect, elevation, relief amplitude, land use, soil type, road distance, geology, fault distance, and rainfall. Furthermore, the model utilizes advanced technologies such as Geographic Information System (GIS), deep learning, and BCMO optimization techniques to integrate various data sources and generate a comprehensive landslide susceptibility map. Besides, LR and SVMachine are used as benchmarks to confirm the proposed model's efficacy. Based on the results of this work, we have arrived at several conclusions below:

- With a combination of the BCMO (Balancing Composite Motion Optimization) algorithm and DeepNeuralNets, a new and effective deep-learning model has been developed to map landslide susceptibility precisely. This

hybrid approach leverages the strengths of both algorithms to achieve higher accuracy in identifying areas that are more susceptible to landslides.

- The performance of the BCMO-DeepNeuralNets outperformed the benchmark models, namely LG and SVMachine; it is a promising new tool for landslide susceptibility mapping. Therefore, it is recommended that the BCMO-DeepNeuralNets model be considered for use in future studies and applications related to landslide susceptibility mapping.
- All landslide-related factors in this research have contributed to landslide occurrence, and among them, slope, distance to roads, and land use are the most prominent factors.
- Landslide susceptibility maps generated from BCMO-DeepNeuralNets can be helpful for policy and decision-making, where appropriate, to mitigate the impact of landslides in the study area.

CONFLICTS OF INTEREST

The authors declare no conflict of interest.

REFERENCES

[1] G. Halkos and A. Zisiadou, "Examining the natural environmental hazards over the last century," *Econ. Disasters Climate Change*, vol. 3, no. 2, pp. 119–150, Jul. 2019.

[2] M. H. Bukhari, P. F. da Silva, J. Pilz, E. Istanbulluoglu, T. Görüm, J. Lee, A. Karamehic-Muratovic, T. Urmi, A. Soltani, W. Wilopo, J. A. Qureshi, S. Zekan, K. S. Koonisetty, U. Sheishenaly, L. Khan, J. Espinoza, E. P. Mendoza, and U. Haque, "Community perceptions of landslide risk and susceptibility: A multi-country study," *Landslides*, vol. 20, pp. 1–14, Feb. 2023.

[3] S. Schneiderbauer, P. F. Pisa, J. L. Delves, L. Pedoth, S. Rufat, M. Erschbamer, T. Thaler, F. Carnelli, and S. Granados-Chahin, "Risk perception of climate change and natural hazards in global mountain regions: A critical review," *Sci. Total Environ.*, vol. 784, Aug. 2021, Art. no. 146957.

[4] J. Zhang, M. Lu, L. Zhang, and Y. Xue, "Assessing indirect economic losses of landslides along highways," *Natural Hazards*, vol. 106, no. 3, pp. 2775–2796, Apr. 2021.

[5] C. Pfurtscheller and E. Genovese, "The Felbertauern landslide of 2013 in Austria: Impact on transport networks, regional economy and policy decisions," *Case Stud. Transp. Policy*, vol. 7, no. 3, pp. 643–654, Sep. 2019.

[6] L. Shano, T. K. Raghuvanshi, and M. Meten, "Landslide susceptibility evaluation and hazard zonation techniques—A review," *Geoenvironmental Disasters*, vol. 7, no. 1, pp. 1–19, Dec. 2020.

[7] C. Yong, D. Jinlong, G. Fei, T. Bin, Z. Tao, F. Hao, W. Li, and Z. Qinghua, "Review of landslide susceptibility assessment based on knowledge mapping," *Stochastic Environ. Res. Risk Assessment*, vol. 36, no. 9, pp. 2399–2417, Sep. 2022.

[8] N. Casagli, F. Catani, C. Puglisi, G. Delmonaco, L. Ermini, and C. Margottini, "An inventory-based approach to landslide susceptibility assessment and its application to the Virginio River Basin, Italy," *Environ. Eng. Geosci.*, vol. 10, no. 3, pp. 203–216, Aug. 2004.

[9] C. J. van Westen, N. Rengers, and R. Soeters, "Use of geomorphological information in indirect landslide susceptibility assessment," *Natural Hazards*, vol. 30, no. 3, pp. 399–419, Nov. 2003.

[10] E. A. Castellanos Abella and C. J. Van Westen, "Qualitative landslide susceptibility assessment by multicriteria analysis: A case study from San Antonio del Sur, Guantánamo, Cuba," *Geomorphology*, vol. 94, nos. 3–4, pp. 453–466, Feb. 2008.

[11] B. Feizizadeh and T. Blaschke, "GIS-multicriteria decision analysis for landslide susceptibility mapping: Comparing three methods for the Urmia lake basin, Iran," *Natural Hazards*, vol. 65, no. 3, pp. 2105–2128, Feb. 2013.

[12] G. Grelle, M. Soriano, P. Revellino, L. Guerriero, M. G. Anderson, A. Diambra, F. Fiorillo, L. Esposito, N. Diodato, and F. M. Guadagno, "Space–time prediction of rainfall-induced shallow landslides through a combined probabilistic/deterministic approach, optimized for initial water table conditions," *Bull. Eng. Geol. Environ.*, vol. 73, no. 3, pp. 877–890, Aug. 2014.

[13] E. Canli, M. Mergili, B. Thiebes, and T. Glade, "Probabilistic landslide ensemble prediction systems: Lessons to be learned from hydrology," *Natural Hazards Earth Syst. Sci.*, vol. 18, no. 8, pp. 2183–2202, Aug. 2018, doi: 10.5194/nhess-18-2183-2018.

[14] P. Reichenbach, M. Rossi, B. D. Malamud, M. Mihir, and F. Guzzetti, "A review of statistically-based landslide susceptibility models," *Earth-Sci. Rev.*, vol. 180, pp. 60–91, May 2018.

[15] S. Das, S. Sarkar, and D. P. Kanungo, "A critical review on landslide susceptibility zonation: Recent trends, techniques, and practices in Indian Himalaya," *Natural Hazards*, vol. 115, no. 1, pp. 23–72, Jan. 2023.

[16] F. S. Tehrani, M. Calvello, Z. Liu, L. Zhang, and S. Lacasse, "Machine learning and landslide studies: Recent advances and applications," *Natural Hazards*, vol. 114, no. 2, pp. 1197–1245, Nov. 2022.

[17] C. Beckham, M. Hall, and E. Frank, "WekaPyScript: Classification, regression, and filter schemes for WEKA implemented in Python," *J. Open Res. Softw.*, vol. 4, no. 1, p. 33, Aug. 2016.

[18] S. Lang, F. Bravo-Marquez, C. Beckham, M. Hall, and E. Frank, "WekaDeeplearning4j: A deep learning package for weka based on Deeplearning4j," *Knowl.-Based Syst.*, vol. 178, pp. 48–50, Aug. 2019.

[19] M. Abadi, P. Barham, J. Chen, Z. Chen, A. Davis, J. Dean, M. Devin, S. Ghemawat, G. Irving, M. Isard, M. Kudlur, J. Levenberg, R. Monga, S. Moore, D. G. Murray, B. Steiner, P. Tucker, V. Vasudevan, P. Warden, M. Wicke, Y. Yu, and X. Zheng, "TensorFlow: A system for large-scale machine learning," in *Proc. OSDI*, Savannah, GA, USA, vol. 16, 2016, pp. 265–283.

[20] E. Haghighat and R. Juanes, "SciANN: A keras/TensorFlow wrapper for scientific computations and physics-informed deep learning using artificial neural networks," *Comput. Methods Appl. Mech. Eng.*, vol. 373, Jan. 2021, Art. no. 113552, doi: 10.1016/j.cma.2020.113552.

[21] L. Bragagnolo, R. V. da Silva, and J. M. V. Grzybowski, "Landslide susceptibility mapping with r.landslide: A free open-source GIS-integrated tool based on artificial neural networks," *Environ. Model. Softw.*, vol. 123, Jan. 2020, Art. no. 104565, doi: 10.1016/j.envsoft.2019.104565.

[22] L. V. Lucchese, G. G. de Oliveira, and O. C. Pedrollo, "Investigation of the influence of nonoccurrence sampling on landslide susceptibility assessment using artificial neural networks," *Catena*, vol. 198, Mar. 2021, Art. no. 105067, doi: 10.1016/j.catena.2020.105067.

[23] G. G. de Oliveira, L. F. C. Ruiz, L. A. Guasselli, and C. Haetinger, "Random forest and artificial neural networks in landslide susceptibility modeling: A case study of the Fão River Basin, Southern Brazil," *Natural Hazards*, vol. 99, no. 2, pp. 1049–1073, Nov. 2019, doi: 10.1007/s11069-019-03795-x.

[24] J. Dou, A. P. Yunus, D. T. Bui, A. Merghadi, M. Sahana, Z. Zhu, C.-W. Chen, Z. Han, and B. T. Pham, "Improved landslide assessment using support vector machine with bagging, boosting, and stacking ensemble machine learning framework in a mountainous watershed, Japan," *Landslides*, vol. 17, no. 3, pp. 641–658, Mar. 2020, doi: 10.1007/s10346-019-01286-5.

[25] B. T. Pham, A. Jaafari, I. Prakash, and D. T. Bui, "A novel hybrid intelligent model of support vector machines and the MultiBoost ensemble for landslide susceptibility modeling," *Bull. Eng. Geol. Environ.*, vol. 78, no. 4, pp. 2865–2886, Jun. 2019, doi: 10.1007/s10064-018-1281-y.

[26] D. T. Bui, T. A. Tuan, H. Klempe, B. Pradhan, and I. Revhaug, "Spatial prediction models for shallow landslide hazards: A comparative assessment of the efficacy of support vector machines, artificial neural networks, kernel logistic regression, and logistic model tree," *Landslides*, vol. 13, no. 2, pp. 361–378, Apr. 2016.

[27] Y. Huang and L. Zhao, "Review on landslide susceptibility mapping using support vector machines," *Catena*, vol. 165, pp. 520–529, Jun. 2018, doi: 10.1016/j.catena.2018.03.003.

[28] H. Hong, J. Liu, D. T. Bui, B. Pradhan, T. D. Acharya, B. T. Pham, A.-X. Zhu, W. Chen, and B. B. Ahmad, "Landslide susceptibility mapping using J48 decision tree with AdaBoost, bagging and rotation forest ensembles in the Guangchang area (China)," *Catena*, vol. 163, pp. 399–413, Apr. 2018, doi: 10.1016/j.catena.2018.01.005.

[29] J. Dou, A. P. Yunus, D. T. Bui, A. Merghadi, M. Sahana, Z. Zhu, C.-W. Chen, K. Khosravi, Y. Yang, and B. T. Pham, "Assessment of advanced random forest and decision tree algorithms for modeling rainfall-induced landslide susceptibility in the Izu-Oshima Volcanic Island, Japan," *Sci. Total Environ.*, vol. 662, pp. 332–346, Apr. 2019, doi: 10.1016/j.scitotenv.2019.01.221.

[30] M. Krkač, S. B. Gazibara, Ž. Arbanas, M. Sečanj, and S. M. Arbanas, "A comparative study of random forests and multiple linear regression in the prediction of landslide velocity," *Landslides*, vol. 17, no. 11, pp. 2515–2531, Nov. 2020, doi: 10.1007/s10346-020-01476-6.

[31] D. Sun, H. Wen, D. Wang, and J. Xu, "A random forest model of landslide susceptibility mapping based on hyperparameter optimization using Bayes algorithm," *Geomorphology*, vol. 362, Aug. 2020, Art. no. 107201, doi: 10.1016/j.geomorph.2020.107201.

[32] Y. Wang, Z. Fang, and H. Hong, "Comparison of convolutional neural networks for landslide susceptibility mapping in Yanshan County, China," *Sci. Total Environ.*, vol. 666, pp. 975–993, May 2019, doi: 10.1016/j.scitotenv.2019.02.263.

[33] W. L. Hakim, F. Rezaie, A. S. Nur, M. Panahi, K. Khosravi, C.-W. Lee, and S. Lee, "Convolutional neural network (CNN) with metaheuristic optimization algorithms for landslide susceptibility mapping in Icheon, South Korea," *J. Environ. Manage.*, vol. 305, Mar. 2022, Art. no. 114367, doi: 10.1016/j.jenvman.2021.114367.

[34] Y. Li, W. Chen, F. Rezaie, O. Rahmati, D. D. Moghaddam, J. Tiefenbacher, M. Panahi, M.-J. Lee, D. Kulakowski, D. T. Bui, and S. Lee, "Debris flows modeling using geo-environmental factors: Developing hybridized deep-learning algorithms," *Geocarto Int.*, vol. 37, no. 17, pp. 5150–5173, Sep. 2022, doi: 10.1080/10106049.2021.1912194.

[35] D. T. Bui, P. Tsangaratos, V.-T. Nguyen, N. V. Liem, and P. T. Trinh, "Comparing the prediction performance of a deep learning neural network model with conventional machine learning models in landslide susceptibility assessment," *Catena*, vol. 188, May 2020, Art. no. 104426, doi: 10.1016/j.catena.2019.104426.

[36] M. Ado, K. Amitab, A. K. Maji, E. Jasinska, R. Gono, Z. Leonowicz, and M. Jasinski, "Landslide susceptibility mapping using machine learning: A literature survey," *Remote Sens.*, vol. 14, no. 13, p. 3029, 2022. [Online]. Available: https://www.mdpi.com/2072-4292/14/13/3029

[37] F. Huang, J. Zhang, C. Zhou, Y. Wang, J. Huang, and L. Zhu, "A deep learning algorithm using a fully connected sparse autoencoder neural network for landslide susceptibility prediction," *Landslides*, vol. 17, no. 1, pp. 217–229, Jan. 2020, doi: 10.1007/s10346-019-01274-9.

[38] K. Mandal, S. Saha, and S. Mandal, "Applying deep learning and benchmark machine learning algorithms for landslide susceptibility modelling in Rorachu river basin of Sikkim Himalaya, India," *Geosci. Frontiers*, vol. 12, no. 5, Sep. 2021, Art. no. 101203, doi: 10.1016/j.gsf.2021.101203.

[39] O. Ghorbanzadeh, T. Blaschke, K. Gholamnia, S. R. Meena, D. Tiede, and J. Aryal, "Evaluation of different machine learning methods and deep-learning convolutional neural networks for landslide detection," *Remote Sens.*, vol. 11, no. 2, p. 196, Jan. 2019. [Online]. Available: https://www.mdpi.com/2072-4292/11/2/196

[40] B. T. Pham, V. D. Vu, R. Costache, T. V. Phong, T. Q. Ngo, T.-H. Tran, H. D. Nguyen, M. Amiri, M. T. Tan, P. T. Trinh, H. V. Le, and I. Prakash, "Landslide susceptibility mapping using state-of-the-art machine learning ensembles," *Geocarto Int.*, vol. 37, no. 18, pp. 5175–5200, Sep. 2022, doi: 10.1080/10106049.2021.1914746.

[41] B. Wang, Q. Lin, T. Jiang, H. Yin, J. Zhou, J. Sun, D. Wang, and R. Dai, "Evaluation of linear, nonlinear and ensemble machine learning models for landslide susceptibility assessment in Southwest China," *Geocarto Int.*, Dec. 2022, Art. no. 2152493, doi: 10.1080/10106049.2022.2152493.

[42] G. Yin, J. Luo, F. Niu, Z. Lin, and M. Liu, "Machine learning-based thermokarst landslide susceptibility modeling across the permafrost region on the Qinghai-Tibet Plateau," *Landslides*, vol. 18, no. 7, pp. 2639–2649, Jul. 2021, doi: 10.1007/s10346-021-01669-7.

[43] M. Di Napoli, F. Carotenuto, A. Cevasco, P. Confuorto, D. Di Martire, M. Firpo, G. Pepe, E. Raso, and D. Calcaterra, "Machine learning ensemble modelling as a tool to improve landslide susceptibility mapping reliability," *Landslides*, vol. 17, no. 8, pp. 1897–1914, Aug. 2020.

[44] T. Le-Duc, Q.-H. Nguyen, and H. Nguyen-Xuan, "Balancing composite motion optimization," *Inf. Sci.*, vol. 520, pp. 250–270, May 2020.

[45] S. Saha, B. Bera, P. K. Shit, S. Bhattacharjee, and N. Sengupta, "Prediction of forest fire susceptibility applying machine and deep learning algorithms for conservation priorities of forest resources," *Remote Sens. Appl., Soc. Environ.*, vol. 29, Jan. 2023, Art. no. 100917.

[46] H. Moon, S. Yoon, and Y. Moon, "Urban flood forecasting using a hybrid modeling approach based on a deep learning technique," *J. Hydroinformatics*, vol. 25, no. 2, pp. 593–610, Mar. 2023.

[47] D. T. Bui, N.-D. Hoang, F. Martínez-Álvarez, P.-T.-T. Ngo, P. V. Hoa, T. D. Pham, P. Samui, and R. Costache, "A novel deep learning neural network approach for predicting flash flood susceptibility: A case study at a high frequency tropical storm area," *Sci. Total Environ.*, vol. 701, Jan. 2020, Art. no. 134413.

[48] A. Mohan, A. K. Singh, B. Kumar, and R. Dwivedi, "Review on remote sensing methods for landslide detection using machine and deep learning," *Trans. Emerg. Telecommun. Technol.*, vol. 32, no. 7, p. e3998, 2021.

[49] K. Shaaban, A. Hamdi, M. Ghanim, and K. B. Shaban, "Machine learning-based multi-target regression to effectively predict turning movements at signalized intersections," *Int. J. Transp. Sci. Technol.*, vol. 12, no. 1, pp. 245–257, Mar. 2023.

[50] V.-T. Tran, T.-K. Nguyen, H. Nguyen-Xuan, and M. Abdel Wahab, "Vibration and buckling optimization of functionally graded porous microplates using BCMO-ANN algorithm," *Thin-Walled Struct.*, vol. 182, Jan. 2023, Art. no. 110267, doi: 10.1016/j.tws.2022.110267.

[51] N. H. Phuong, P. T. Truyen, and N. T. Nam, "Probabilistic seismic hazard assessment for the Tranh river hydropower plant No2 site, Quang Nam province," *Vietnam J. EARTH Sci.*, vol. 38, no. 2, pp. 188–201, Aug. 2016, doi: 10.15625/0866-7187/38/2/8601.

[52] L. Q. Hung, N. T. H. Van, P. V. Son, N. H. Ninh, N. Tam, and N. T. Huyen, "Landslide inventory mapping in the fourteen Northern provinces of Vietnam: Achievements and difficulties," in *Advancing Culture of Living With Landslides*, K. Sassa, M. Mikoš, and Y. Yin, Eds. Cham, Switzerland: Springer, 2017, pp. 501–510.

[53] N. Q. Thanh, N. T. Yem, T. T. Anh, N. T. Phuong, N. T. Cau, N. D. Ngu, N. T. Hieu, H. V. Dai, T. H. Thai, N. T. Cong, N. L. Minh, N. V. Hoang, V. T. H. Lien, N. V. Tien, T. A. Tuan, N. T. Tai, N. T. Kien, N. V. Hung, B. V. Thom, and D. T. Hau, "To study, supplement and develop a map of natural disasters in Vietnam's mainland based on research results from 2000 up to now," Inst. Geological Sci., Vietnam Acad. Sci. Technol., Hanoi, Vietnam, Rep. KC.08.28/11-15, 2015.

[54] M. T. Tan, V. V. Ha, N. T. Tan, H. Q. Vinh, N. V. Liem, L. D. Luong, T. T. Ha, N. V. Tao, H. L. T. Thuy, L. T. Anh, and T. T. T. Van, "Landslide hazard assessment by geological and geomorphological methods integrated with the GIS optimal weighting model in river basins in Thua Thien Hue, Quang Nam, and Da Nang areas, proposing solutions prevent," Inst. Geol. Sci., Vietnam Acad. Sci. Technol., Hanoi, Vietnam, Tech. Rep. VAST 09.01/11-12, 2014.

[55] R. Anbalagan, "Landslide hazard evaluation and zonation mapping in mountainous terrain," *Eng. Geol.*, vol. 32, no. 4, pp. 269–277, Jul. 1992, doi: 10.1016/0013-7952(92)90053-2.

[56] D. W. Allen and J. M. Coffey, *Focus on Geodatabases in ArcGIS Pro*. Redlands, CA, USA: Esri Press, 2019.

[57] M. Mergili, I. Marchesini, M. Alvioli, M. Metz, B. Schneider-Muntau, M. Rossi, and F. Guzzetti, "A strategy for GIS-based 3-D slope stability modelling over large areas," *Geosci. Model Develop.*, vol. 7, no. 6, pp. 2969–2982, Dec. 2014.

[58] A. Cardenas-Martinez, V. Rodriguez-Galiano, J. A. Luque-Espinar, and M. P. Mendes, "Predictive modelling benchmark of nitrate vulnerable zones at a regional scale based on machine learning and remote sensing," *J. Hydrol.*, vol. 603, Dec. 2021, Art. no. 127092, doi: 10.1016/j.jhydrol.2021.127092.

[59] P. V. Gorsevski, "A free web-based approach for rainfall-induced landslide susceptibility modeling: Case study of clearwater national forest, Idaho, USA," *Environ. Model. Softw.*, vol. 161, Mar. 2023, Art. no. 105632.

[60] A. Merghadi, A. P. Yunus, J. Dou, J. Whiteley, B. ThaiPham, D. T. Bui, R. Avtar, and B. Abderrahmane, "Machine learning methods for landslide susceptibility studies: A comparative overview of algorithm performance," *Earth-Sci. Rev.*, vol. 207, Aug. 2020, Art. no. 103225, doi: 10.1016/j.earscirev.2020.103225.

[61] G. Jia, M. Alvioli, S. L. Gariano, I. Marchesini, F. Guzzetti, and Q. Tang, "A global landslide non-susceptibility map," *Geomorphology*, vol. 389, Sep. 2021, Art. no. 107804.

[62] C.-J.-F. Chung and A. G. Fabbri, "Validation of spatial prediction models for landslide hazard mapping," *Natural Hazards*, vol. 30, no. 3, pp. 451–472, Nov. 2003.

[63] K. B. Sim, M. L. Lee, and S. Y. Wong, "A review of landslide acceptable risk and tolerable risk," *Geoenvironmental Disasters*, vol. 9, no. 1, p. 3, Dec. 2022.

[64] W. Shabbir, T. Omer, and J. Pilz, "The impact of environmental change on landslides, fatal landslides, and their triggers in Pakistan (2003–2019)," *Environ. Sci. Pollut. Res.*, vol. 30, no. 12, pp. 33819–33832, 2023.
[65] W. Zhang, X. Gu, L. Tang, Y. Yin, D. Liu, and Y. Zhang, "Application of machine learning, deep learning and optimization algorithms in geoengineering and geoscience: Comprehensive review and future challenge," *Gondwana Res.*, vol. 109, pp. 1–17, Sep. 2022.
[66] H. S. Munawar, M. Mojtahedi, A. W. A. Hammad, A. Kouzani, and M. A. P. Mahmud, "Disruptive technologies as a solution for disaster risk management: A review," *Sci. Total Environ.*, vol. 806, Feb. 2022, Art. no. 151351.
[67] D. T. Bui, T. A. Tuan, N.-D. Hoang, N. Q. Thanh, D. B. Nguyen, N. Van Liem, and B. Pradhan, "Spatial prediction of rainfall-induced landslides for the Lao Cai area (Vietnam) using a hybrid intelligent approach of least squares support vector machines inference model and artificial bee colony optimization," *Landslides*, vol. 14, no. 2, pp. 447–458, Apr. 2017.
[68] L. N. Thanh and F. De Smedt, "Application of an analytical hierarchical process approach for landslide susceptibility mapping in A Luoi district, Thua Thien Hue Province, Vietnam," *Environ. Earth Sci.*, vol. 66, no. 7, pp. 1739–1752, Aug. 2012.
[69] C. Luu and J. von Meding, "A flood risk assessment of Quang Nam, Vietnam using spatial multicriteria decision analysis," *Water*, vol. 10, no. 4, p. 461, Apr. 2018.
[70] V. N. Chau, S. Cassells, and J. Holland, "Economic impact upon agricultural production from extreme flood events in Quang Nam, central Vietnam," *Natural Hazards*, vol. 75, no. 2, pp. 1747–1765, Jan. 2015.
[71] H. T. L. Huynh, L. N. Thi, and N. D. Hoang, "Assessing the impact of climate change on agriculture in Quang Nam Province, Viet Nam using modeling approach," *Int. J. Climate Change Strategies Manage.*, vol. 12, no. 5, pp. 757–771, Dec. 2020.

TRAN ANH TUAN received the Ph.D. degree in management of resources and environment from the University of Sciences, Vietnam National University, Hanoi, in 2016. He is currently a Mid-Tier Researcher and the Head of the Remote Sensing and GIS Department, Institute of Marine Geology and Geophysics, Vietnam Academy of Science and Technology. His research interests include basic research on geomorphology, natural geographic zoning, applied remote sensing and GIS for natural hazards, and integrated assessment for development purposes.

PHAN DONG PHA received the bachelor's degree in geography-geology from Hanoi University (now the University of Sciences, Vietnam National University, Hanoi), in 1983, and the master's and Ph.D. degrees in geology from the Hanoi University Mining and Geology, in 2004 and 2012, respectively, with a focus on paleontology-stratigraphy, sedimentology, geological hazards, and exogenous minerals.

From 1984 to 2012, he was a Researcher with the Institute of Geological Sciences, Vietnam Academy of Science and Technology (VAST). Since 2007, he has been a Senior Researcher and the Head of the Department of Marine Geomorphology and Paleogeography, Institute of Marine Geology and Geophysics, VAST. He is the author and coauthor of one book and about 100 articles. His research interests include Cenozoic sedimentary stratigraphy, the evolutionary history of cenozoic sedimentary basins, and geological hazards (landslides, flash floods, and debris flows).

Dr. Pha has been a member of the General Association of Geology of Vietnam, the Association of Geomorphology-Quaternary Vietnam, and the Association of Paleontology and Stratigraphy of Vietnam, since 1984.

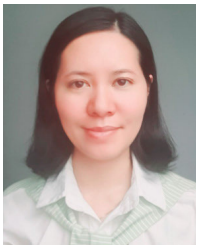

TRAN THI TAM received the bachelor's and master's degrees in geography from the University of Sciences, Vietnam National University, Hanoi, in 2008 and 2014, respectively. From 2008 to 2010, she was a Researcher with the Department of Mapping, Remote Sensing, and GIS Research, Vietnam Institute of Meteorology, Hydrology and Climate Change (IMHEN), Vietnam. Since 2010, she has been a Researcher with the Research Center for Agro-Meteorology, IMHEN. Her research interests include GIS and geospatial information science, remote sensing, forecasting the yield and growth of crops, agro-climatic zoning, climate modeling, and the impact assessment of disasters and extreme weather events.

DIEU TIEN BUI is currently a Full Professor with the GIS Group, Department of Business and IT, University of South-Eastern Norway (USN), Norway. He has more than 200 publications, and out of them, more than 180 articles were published in science citation index (SCI/SCIE) indexed journals. His research interests include GIS and geospatial information science, remote sensing, and applied artificial intelligence and machine learning for natural hazards and environmental problems, such as landslide, flood, forest fire, ground biomass, and structural displacement.